ELSEVIER

Catalysis Today 71 (2001) 121–128

CATALYSIS TODAY

www.elsevier.com/locate/cattod

Correlation with the redox V^{5+}/V^{4+} ratio in vanadium phosphorus oxide catalysts for mild oxidation of *n*-butane to maleic anhydride

M. Abon [a], J.M. Herrmann [b], J.C. Volta [a,*]

[a] *Institut de Recherches sur la Catalyse, CNRS, 2 Avenue Albert Einstein, 69626 Villeurbanne Cedex, France*

[b] *Laboratoire de Photocatalyse, Catalyse et Environnement, CNRS (IFOS), Ecole Centrale de Lyon, BP 163, 69131 Ecully Cedex, France*

Abstract

The redox properties of vanadium phosphorus oxide (VPO) catalysts have been compared to their catalytic performance in fuel-lean conditions for two sets of $(VO)_2P_2O_7$ catalysts obtained after calcination under nitrogen at different temperatures or after different postoxidation periods under dioxygen. It is shown that doping the VPO catalysts with Co and Mo makes possible for the catalyst to produce maleic anhydride in fuel-rich conditions. In both situations, catalytic performances are dependent on the vanadium oxidation state of the catalysts. © 2001 Published by Elsevier Science B.V.

Keywords: *n*-Butane; Maleic anhydride; Vanadium phosphorus oxides; Doping

1. Introduction

Vanadium phosphorus oxide (VPO) is the typical catalyst for mild oxidation of *n*-butane to maleic anhydride. For this catalyst, vanadyl pyrophosphate $(VO)_2P_2O_7$ is considered as the bulk phase of the long term 'equilibrated' industrial VPO catalyst, since it is the only phase identified by X-ray diffraction. The VPO catalyst is obtained after a progressive transformation of the vanadyl phosphohemihydrate $VOHPO_4{\cdot}0.5H_2O$ precursor to $(VO)_2P_2O_7$ by dehydration. However, the final catalytic performance of the VPO catalyst depends on the succession of surface and bulk transformations, the relative importance of which differ with the conditions of activation of the precursor. During this period, there is an evolution of the acido-basic properties and a variation of the oxidation state of vanadium which affects both the surface and the bulk.

In the present paper, it is shown that the catalytic performance of the VPO catalyst may be controlled by the oxidation state of vanadium through the surface V^{5+}/V^{4+} ratio necessary for the mild oxidation of *n*-butane to maleic anhydride, in agreement with the rules of the Mars–van Krevelen mechanism [1].

2. Experimental

Three series of experiments have been conducted independently in order to modify the surface and bulk composition of the VPO catalysts and to study the influence on the catalytic performance.

In the two series, VPO catalysts were prepared from the same $VOHPO_4{\cdot}0.5H_2O$ precursor obtained according to the Exxon organic route. The conditions of preparation of these precursors have been previously published [2,3]. The VPO precursors were then submitted to different conditions of activation to change the characteristics of the final VPO catalysts by calcination and oxidation:

* Corresponding author. Tel.: +33-4-72-44-53-14; fax: +33-4-72-44-53-99.
E-mail address: volta@catalyse.univ-lyon1.fr (J.C. Volta).

0920-5861/01/$ – see front matter © 2001 Published by Elsevier Science B.V.
PII: S0920-5861(01)00434-5

- In a first series of experiments, the precursor was calcined under N_2 at temperatures from 450 up to 880°C.
- In a second series of experiments, the standard $(VO)_2P_2O_7$ calcined at 750°C under N_2 and denoted (PYRO) was heated up to 500°C (5°C/min) under an oxygen flow (20 ml/min) and then kept at this temperature from 0.5 to 24 h. This series of preoxidized catalysts is denoted as PYRO-OX.

For these two series, the VPO catalysts were then compared for *n*-butane oxidation to maleic anhydride at 380–400°C in a flow microreactor working at atmospheric pressure, in fuel-lean conditions, with the gas mixture composition: $nC_4/O_2/He = 1.6/18/80.4$ – GSHV = 1500 h^{-1}.

In the third series of experiments, the VPO precursors were prepared by reduction of $VOPO_4{\cdot}2H_2O$ with isobutanol (VPD route) [4]. The VPO precursors were then modified by doping, according to two different routes:

- Introduction of the Co dopant as Co acetylacetonate into isobutanol prior to the reduction of $VOPO_4{\cdot}2H_2O$.
- Impregnation of the ammonium heptamolybdate, once the $VOHPO_4{\cdot}0.5H_2O$ precipitated.

For this third series, the VPO catalysts were then compared for *n*-butane oxidation to maleic anhydride at 400°C in a flow microreactor working at atmospheric pressure, in fuel-rich conditions, with the gas mixture composition: $nC_4/O_2/He = 16.6/10/73.4$ – GSHV = 3000 h^{-1}. For all the catalytic tests, on-line analysis of reactants and products was achieved by gas chromatography using three different columns to separate hydrocarbons, oxygenates and CO_x. Sampling valves and tubing were located into a hot box (140°C). The carbon mass balance obtained was better than 97–98%.

In both fuel-lean and fuel-rich conditions, performances were measured at stationary state. Catalysts were denoted VPDCo, VPDMo1, VPDMo2 and VPDMo3 with the corresponding composition Co/V = 0.77, Mo/V = 0.83, 1.21 and 2.56, respectively.

^{31}P NMR by spin-echo mapping and XPS were used as physicochemical techniques to get crossed information on the relative distribution of V^{4+} and V^{5+} species in the bulk and at the surface of the VPO catalysts. ^{31}P NMR spectra were recorded on a Bruker DSX 400 spectrometer operating at 161.9 MHz, using a 4 mm standard probe head. Spectra were obtained at a spinning speed of 12 kHz with a pulse length of 1.5 μs and a recycle delay of 60 s. XPS analysis was performed in a VG Escalab 200R model using the Mg Kα radiation. The relative percentage of surface V^{4+} and V^{5+} species has been estimated (at ca. 10%) from the V $2p_{3/2}$ peak using a peak deconvolution and curve fitting technique. Electron conductivity measurements have been used to study the electronic interactions between some of the powdered VPO samples and *n*-butane, O_2, *n*-butane/O_2 catalytic gas mixture. A specially designed cell was used for these studies [5]. The electrical conductivity of the pyrophosphate samples was measured at 400°C under O_2 (16.7 kPa), *n*-butane (1.47 kPa) and the reaction mixture (O_2/C_4 = 125/11) in order to simulate the fuel-lean conditions of the test.

3. Results and discussion

3.1. Comparison of pyrophosphate (PYRO) VPO catalysts precalcined at different temperatures under N_2

As observed by X-ray diffraction, the crystallinity of the VPO catalysts increases with the temperature of calcination. A progressive shift of the characteristic signal of V^{4+} in $(VO)_2P_2O_7$ is observed in the ^{31}P NMR signal by spin-echo mapping from 2500 ppm for PYRO 450 up to 2630 ppm for PYRO 880 (Fig. 1). Signal near 0 ppm, which is almost absent for calcination at 750 and 880°C, has been explained by the presence of superficial V^{5+} species for low temperatures of calcination. This information is confirmed by the XPS studies: the decomposition of the V $2p_{3/2}$ peak between two contributions at 516.9 eV (V^{4+}) and 518 eV (V^{5+}) allows a measurement of the V^{4+}/V^{5+} ratio at the surface. In Fig. 2, it is observed that the intrinsic activity to MA, measured in fuel-lean conditions at 400°C, reaches a maximum for the VPO calcined at 750°C for which the V^{4+}/V^{5+} ratio is around 6–7.

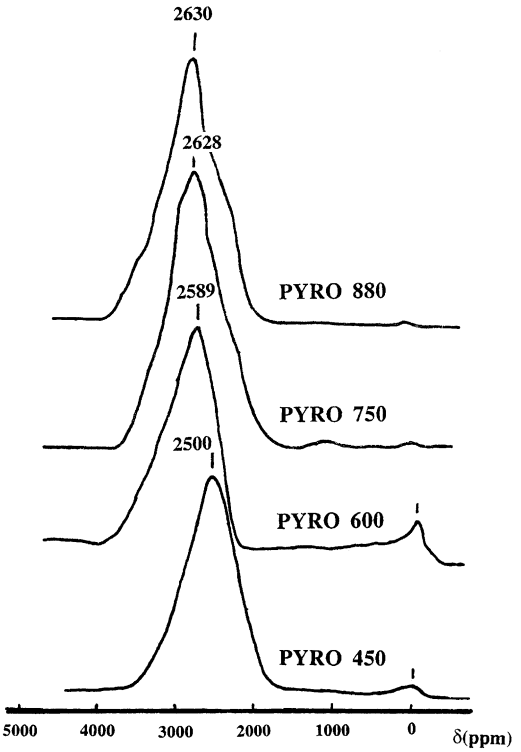

Fig. 1. ^{31}P NMR spectra by spin-echo mapping as a function of the temperature of calcination.

3.2. Comparison of pyrophosphate (PYRO) catalysts preoxidized at different times under O_2

From the previous study it was found that the intrinsic activity in MA formation of $(VO)_2P_2O_7$ catalysts calcined under N_2 at different temperatures is strongly dependent on the surface V^{4+}/V^{5+} ratio as measured by XPS. Another possibility of changing this ratio, and thus the catalytic activity, is to oxidize the $(VO)_2P_2O_7$ catalyst by a pretreatment in O_2. It is what occurs in the regenerator of the recirculating riser reactor used in the DuPont process [6,7].

Fig. 3 shows the variations of selectivity in MA at 10–12% *n*-butane conversion for PYRO and PYRO-OX catalysts, depending on the time of O_2 pretreatment [8]. A strong increase of selectivity in MA from 52% for PYRO up to 84% for PYRO-OX-1 is observed with a maximum and a further decrease down to 75% for PYRO-OX-24. After hot water leaching (HWL), MA selectivity decreases to 60%, a value higher than observed for the original PYRO sample (52%). Different physicochemical investigations of the catalysts have been conducted in order to explain the modification of the catalytic performance [9].

In the ^{31}P NMR spin-echo mapping spectra, apart from the signal in the 2000–3000 ppm range,

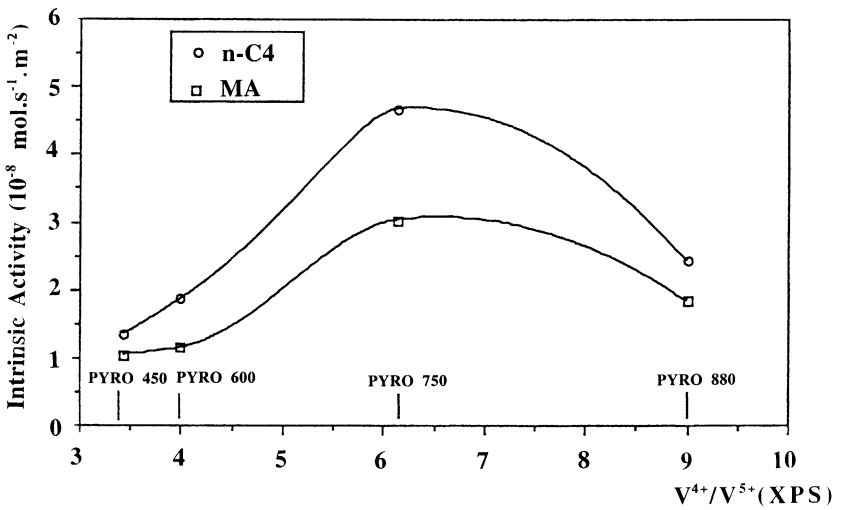

Fig. 2. Influence of the V^{4+}/V^{5+} (XPS ratio on intrinsic activities for nC_4 conversion and MA formation on PYRO catalysts precalcined at different temperatures under N_2.

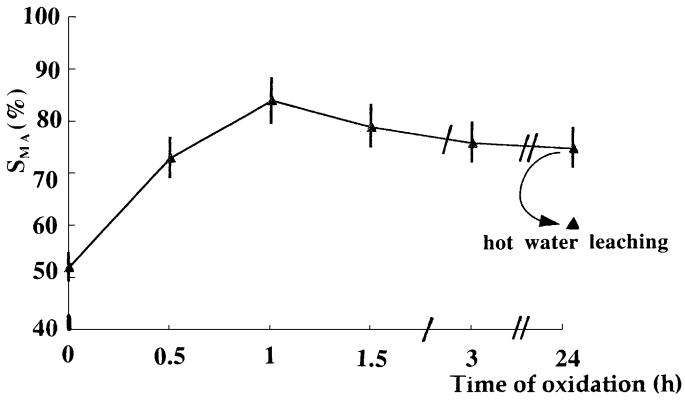

Fig. 3. Influence of an O_2 oxidation pretreatment on MA selectivity in nC_4 mild oxidation.

characteristic of V^{4+} surrounding P atoms in $(VO)_2P_2O_7$, two signals are observed around 0 ppm: a first one at 90 ppm and a more complex one, with a maximum at −25 ppm (Fig. 4). These two last signals are typical of P atoms in a V^{5+} environment. Signal at 90 ppm increases from PYRO-OX-1 up to PYRO-OX-24 comparatively to signal at −25 ppm. After HWL, signal at 90 ppm disappears, which evidences that this signal is connected to the equivalent of some $VOPO_4$ phase (solubilized in hot water) or to a high degree of condensation of the V^{5+} species. From these considerations, it is proposed that these two signals are, respectively, connected to V^{5+} microdomains (signal at 90 ppm) and to V^{5+} isolated sites (complex signal at −25 ppm). These proposals are confirmed by the examination of the same solids by ^{31}P MAS NMR (Fig. 5). Indeed, the corresponding

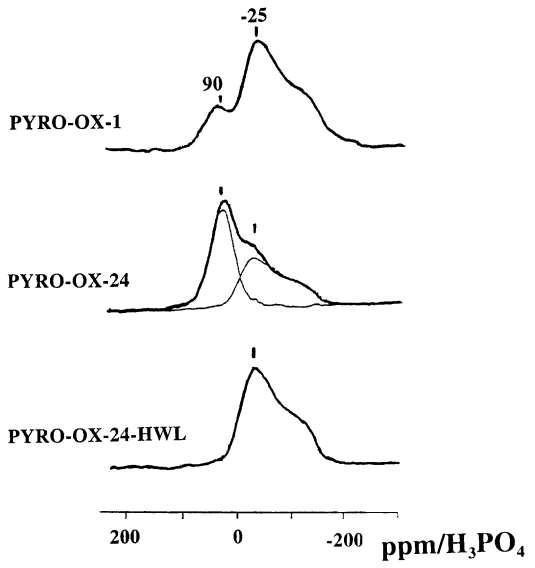

Fig. 4. Variation of the ^{31}P NMR spin-echo mapping spectra of samples preoxidized in O_2 for 1 and 24 h (PYRO-OX-1 and PYRO-OX-24) and after HWL (PYRO-OX-24-HWL).

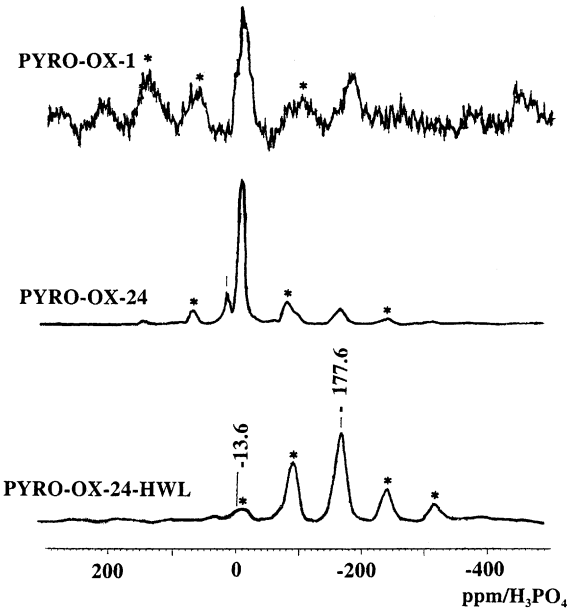

Fig. 5. Variation of the ^{31}P NMR spin-echo mapping spectra with time O_2. Time is expressed in hours — HWL: after HWL treatment.

spectra show also two main contributions: at −13.6 and −177.6 ppm. The intensity of their associated rotating bands evidences a high dispersion of the V^{5+} species around P atoms in the case of the signal at −177.6 ppm (isolated V^{5+} sites), which is not the case for the signal at −13.6 ppm (V^{5+} microdomains).

The different relative distribution between isolated V^{5+} sites and V^{5+} microdomains in the PYRO-OX catalysts is the reason for differences observed in MA selectivity of the corresponding catalysts in C_4 mild oxidation. It is quite interesting to note that PYRO-OX-24-HWL, for which V^{5+} microdomains have been eliminated and for which only isolated V^{5+} species are present, has a higher MA selectivity (60%) as compared to the initial PYRO (MA selectivity 52%) for which they are absent.

The changes in electron conductivity (σ) for this p-type semiconductor give interesting information on the differences observed in the physicochemistry of the vanadyl pyrophosphate catalysts (isolated V^{5+} sites and V^{5+} microdomains) when contacting the reacting gases [9]. Results are presented in Fig. 6a and b. Let us comment on the evolution of σ.

3.2.1. PYRO-OX-3-HWL catalyst as compared to PYRO catalyst

The ^{31}P NMR study has shown that the difference between these two catalysts is the presence of isolated V^{5+} species for PYRO-OX-3-HWL since HWL has eliminated the V^{5+} microdomains which are absent for PYRO (Fig. 6a).

For PYRO, the introduction of C_4 results in a strong decrease of σ, as a result of the reduction of $(VO)_2P_2O_7$ by *n*-butane affecting the O^{2-} species of the surface (bc) and in conformity with its p-type semiconductivity. This initial period under static nC_4 is followed by a progressive increase of σ, due to the diffusion to the surface of the O^{2-} species from the sublayers (cd).

For PYRO-OX-3-HWL, the σ decrease at nC_4 introduction (qr) is very similar to that of PYRO, which demonstrates that the initial reduction effect on this catalyst by nC_4 is not affected by the presence of isolated V^{5+} species. The similitude of these two catalysts is confirmed by the almost similar values of σ before the initial exposure to nC_4. However, differences in σ appear between PYRO-OX-3-HWL and PYRO for the period of diffusion to the surface of the O^{2-} species from the sublayers (rs section for PYRO-OX-3-HWL versus section cd for PYRO). Indeed, the increase in σ is much lower for PYRO-OX-3-HWL. This could be due to a slower diffusion of O^{2-} species delayed by the presence of the V^{5+} isolated sites in the sublayers of the pyrophosphate material.

For PYRO and PYRO-OX-3-HWL, the introduction of O_2 causes a rapid and similar increase of σ for both catalysts. A maximum is observed within a few minutes. It may be explained by the reoxidation of the surface layers which have been previously reduced in the C_4 sequence. The further increase (sections ef and tu), very similar for both catalysts, is explained, as previously, by the diffusion of the O^{2-} species of the sublayers.

The introduction of the ($nC_4H_{10}+O_2$) reaction mixture results in a reduction of both catalysts, which is less pronounced as compared to the C_4 sequence. The rapid decrease for PYRO-OX-3-HWL (section uv) is indicative of the absence of any V^{5+} microdomains on this catalyst, in contrast with PYRO for which the V^{5+} microdomains appear to have been restored after the previous O_2 sequence: the fg section of the σ curve is indicative of their reduction under (C_4/O_2) atmosphere. Another interesting information is that the presence of isolated V^{5+} species has impeded the growth of the V^{5+} microdomains during the previous O_2 sequence for PYRO-OX-3-HWL.

3.2.2. PYRO-OX-1 catalyst as compared to PYRO catalyst

The ^{31}P NMR study has shown that the difference between these two catalysts is the presence of both V^{5+} microdomains and isolated V^{5+} species for PYRO-OX-1 which are both absent in PYRO (Fig. 6b).

PYRO-OX-1 presents a higher σ as compared to PYRO. This is due to the presence of the V^{5+} microdomains on this catalyst since isolated V^{5+} species which are also present on PYRO-OX-1 do not result in any change of σ (see Fig. 6a). This is also in line with a promoted p-type semiconductivity induced by the oxidizing treatment.

The introduction of nC_4 on PYRO-OX-1 results in a low decrease (jk) of σ as compared to PYRO for which it is very fast (bc). This low decrease is indicative of the reduction of the superficial V^{5+} microdomains which are primarily affected. The lm part of the σ

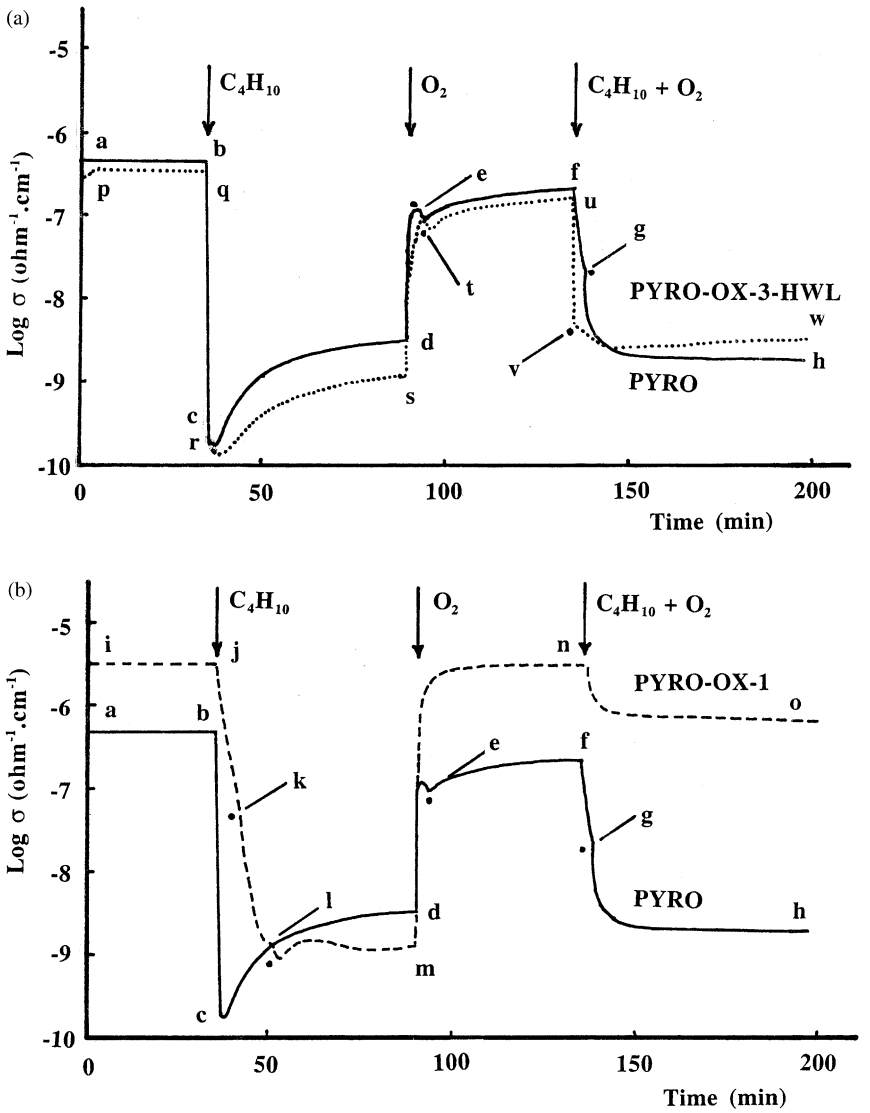

Fig. 6. (a) Kinetics of variation of the electrical conductivity of PYRO (solid line) and PYRO-OX-3-HWL (dotted line) catalysts for various sequences in nC$_4$, O$_2$ and (nC$_4$ + O$_2$) reaction mixtures. (b) Kinetics of variation of the electrical conductivity of PYRO (solid line) and PYRO-OX-1 (dotted line) catalysts for various sequences in nC$_4$, O$_2$ and (nC$_4$ + O$_2$) reaction mixture.

curve is due to the diffusion of the O^{2-} species of the sublayers, as previously discussed.

After O_2 introduction, σ increases because of the growth of the V^{5+} microdomains. In this case, the O^{2-} diffusion appears to be much more rapid for PYRO-OX-1 as compared to PYRO which is a high specificity of this catalyst. This specificity of PYRO-OX-1 is further confirmed when compared to PYRO since the introduction of ($C_4 + O_2$) induces a much lower decrease of σ, which is indicative of a higher oxidability of PYRO-OX-1 as compared to PYRO.

In conclusion on the electrical conductivity data, the most active vanadyl pyrophosphate catalysts are those in the oxidized state. This is in line with the p-type semiconductivity [10]. This requires that the electric

Table 1
Catalytic results obtained at 400°C for nC_4 mild oxidation in fuel-rich conditions ($nC_4/O_2/He = 16.6/10/73.4$ – GSHV = $3000\,h^{-1}$)

Catalyst	Catalytic results (%)							IA_{MA} (10^{-5} mol m^{-2} h^{-1})	S_{BET} (m^2 g^{-1})
	$C(C_4H_{10})$	$C(O_2)$	S_{MA}	$S_{C_4H_8}$	S_{CO}	S_{CO_2}	Y_{MA}		
VPD	15.5	100	0	45.1	32.8	5	0	0	17.1
VPDCo	25.5	77.9	11.5	42	22.4	23.8	2.9	4.62	28.0
VPDMo1	16	96.5	5.7	47.2	26.6	20.5	0.9	1.28	16.5
VPDMo2	8.2	81	8.3	33.7	30.7	27.3	0.7	1.34	17.5
VPDMo3	5.3	63.2	36.5	1.1	28.8	33.8	1.9	3.25	21.9

charge are positive holes h^+ directly related to the presence of isolated V^{5+} atoms in vanadyl position.

$$(V^{V}O)^{3+} \Leftrightarrow (V^{IV}O)^{2+} + h^+$$

Holes h^+, which are electronic vacancies, chemically correspond to O^- species according to:

$$V^{5+} + O^{2-} \Leftrightarrow V^{4+} + O^-$$

These oxidizing species are probably those which are not only able to oxydehydrogenate butane, but also to insert into butene $C_4^=$ molecules, giving birth to maleic anhydride. p-Type semiconductivity implies an excess $\frac{1}{2}\varepsilon$ of oxygen anions, which is the source of oxygen atoms transferred to MA formation

$$(V^{IV}O)_2P_2O_7 + \tfrac{1}{4}\varepsilon \Leftrightarrow (V^{IV}O)_{2-\varepsilon}(V^{V}O)_{\varepsilon}P_2O_{7+\varepsilon/2}$$

3.3. Adaptation by doping of pyrophosphate VPO catalysts to fuel-rich oxidation conditions

The mild oxidation of *n*-butane to maleic anhydride on the VPO catalysts is usually performed in fuel-lean conditions. When turning from fuel-lean conditions ($O_2/C_4 = 12$) to fuel-rich conditions ($O_2/C_4 = 0.6$), it was observed that the VPO catalyst deactivates in a few hours and does not produce any more maleic

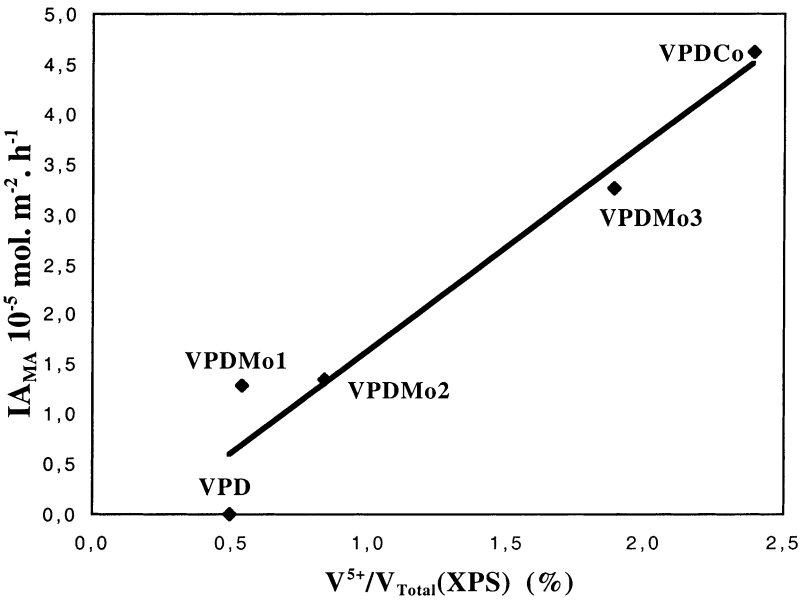

Fig. 7. Correlation between intrinsic activity in MA formation and XPS V^{5+}/V_{total} (%) ratio for VPO-doped catalysts used for nC_4 mild oxidation in fuel-rich conditions ($O_2/C_4 = 0.6$).

anhydride [11]. This deactivation in fuel-rich conditions is not so drastic when the VPO catalyst has been previously preactivated by O_2 at low temperature (500°C), but it still occurs after a longer time [11]. By XPS, it was demonstrated that the O_2 pretreatment initially induces an increase of the surface V^{5+} percentage on the PYRO catalyst. However, deactivation for MA production finally occurs and only butenes isomers and 1–3 butadiene are subsequently produced. This is explained, in such fuel-rich conditions, by the impossibility for the V^{5+} sites, which are in lower density, to insert O in the C_4 molecular intermediates to produce maleic anhydride.

We subsequently tried to reinforce the oxidative capacity of the VPO catalyst for the production of maleic anhydride by using Co and Mo as dopants. VPO precursors prepared according to the third series of preparation (see Section 2) were used and tested in fuel-rich conditions [12]. No deactivation of the Co–VPO catalyst was confirmed after the test in fuel-rich conditions by the observation in the corresponding ^{31}P NMR spectrum of the characteristic signal of the V^{5+} species at 0 ppm, which was not the case for the undoped VPO. Catalytic results are presented in Table 1.

In such fuel-rich conditions, a good correlation was observed between intrinsic activity in MA and the V^{5+}/V_{total} ratio, as measured by XPS after reaction, which evidences that doping controls the final chemical steps to maleic anhydride in the reaction scheme (Fig. 7).

4. Conclusions

The reactivity of the VPO catalysts for mild oxidation of *n*-butane is controlled by the oxidation state of vanadium at the surface which can be regulated according to the different pretreatments of the catalyst. *n*-Butane molecules are activated on acidic centers (V^{4+} sites with ionic vacancies) (first step). Simultaneously, V^{5+} sites are responsible for the p-type semiconductivity of the pyrophosphate, i.e. of some excess oxygen anions. Some of these species will participate in the subsequent O insertion steps into the $C_4^{=}$ intermediates to give birth to maleic anhydride. The V^{5+}/V^{4+} ratio is observed for the intrinsic activity to maleic anhydride. A precalcination in O_2 of the vanadyl pyrophosphate catalyst favors selectivity to maleic anhydride. The existence of isolated V^{5+} sites and V^{5+} microdomains has been evidenced by ^{31}P NMR. Their respective location in the VPO material has been studied via the study of the variation of the electron conductivity when interacting with C_4 and O_2: it has been concluded that V^{5+} microdomains are located at the surface while isolated V^{5+} sites are located in sublayers of the vanadyl pyrophosphate structure. The fuel-lean (i.e. oxidizing) conditions of reaction ($O_2/C_4 = 12$) allows to maintain the V^{5+}/V^{4+} ratio at an optimal value (near 0.25) which corresponds to one V^{5+} site for four V^{4+} sites. These conditions are not any more valid in fuel-rich conditions (i.e. reducing) ($O_2/C_4 = 0.6$). In this case, the only possibility to allow the VPO catalyst to work for mild oxidation of *n*-C_4 to maleic anhydride is to add a dopant into the VPO material. The nature of dopants, their optimal concentrations and their localization are still under investigation, but it has been observed that Co and Mo are suitable for helping VPO catalyst to work in fuel-rich conditions.

References

[1] P. Mars, D.W. van Krevelen, Chem. Eng. Sci. (special Suppl.) 3 (1954) 41.
[2] T.C. Yang, K.K. Rao, I. Der Huan, US Patent 4 392 986 (1987), Exxon Res. Eng. Co.
[3] J.W. Johnson, D.C. Johnston, A.C. Jacobson, J.F. Brody, J. Am. Chem. Soc. 106 (1984) 8123.
[4] C.J. Kiely, A. Burrows, S. Sajip, G.J. Hutchings, M.T. Sananès, A. Tuel, J.C. Volta, J. Catal. 162 (1996) 31.
[5] J.M. Herrmann, in: B. Imelik, J.C. Védrine (Eds.), Catalyst Characterization, Physical Techniques for Solid Materials, Plenum Press, New York, 1994, p. 559 (Chapter 20).
[6] R.M. Contractor, US Patent 4 668 802 (1987), E.I. Du Pont de Nemours.
[7] R.M. Contractor, D.I. Garnett, H.S. Horowitz, H.E. Bergna, G.S. Patience, J.T. Schwartz, G.M. Sisler, New developments in selective oxidation II, Stud. Surf. Sci. Catal. 82 (1994) 233.
[8] K. Aït Lachgar, M. Abon, J.C. Volta, J. Catal. 171 (1997) 383.
[9] K. Aït Lachgar, A. Tuel, M. Brun, J.M. Herrmann, J.M. Krafft, J.R. Martin, J.C. Volta, M. Abon, J. Catal. 177 (1998) 224.
[10] J.M. Herrmann, P. Vernoux, K. Béré, M. Abon, J. Catal. 167 (1997) 106.
[11] S. Mota, M. Abon, J.C. Volta, J.A. Dalmon, J. Catal. 193 (2000) 308.
[12] S. Mota, J.C. Volta, G. Vorbeck, J.A. Dalmon, J. Catal. 193 (2000) 319.